Concomitant *EGFR* Mutation and *EML4-ALK* Rearrangement in Lung Adenocarcinoma Is More Frequent in Multifocal Lesions

Jun Fan,[1] Xiaofang Dai,[2] Zhenkao Wang,[1] Bo Huang,[1] Heshui Shi,[3] Danju Luo,[1] Jiwei Zhang,[1] Weijing Cai,[4] Xiu Nie,[1] Fred R. Hirsch[5]

Abstract

We retrospectively investigated the intertumoral heterogeneity of pathologic and genetic characteristics of multifocal lung adenocarcinomas (LUAC) with epidermal growth factor receptor (*EGFR*)/anaplastic lymphoma kinase (*ALK*) co-alterations. The prevalence of *EGFR*/*ALK* co-alterations was higher in the multifocal LUAC than in the unifocal LUAC. To determine appropriate treatment strategies, extensive molecular profiling could give us more information to distinguish primary lesions from metastatic lesions.

Background: The coexistence of epidermal growth factor receptor (*EGFR*) mutation and anaplastic lymphoma kinase (*ALK*) rearrangement in patients with multifocal lung adenocarcinomas (LUAC) constitutes a rare molecular subtype of lung cancer. We aimed to investigate the intertumoral heterogeneity of pathologic and genetic characteristics of multifocal LUAC with *EGFR*/*ALK* co-alterations. **Patients and Methods:** A total of 1059 LUAC patients who underwent resection were investigated to screen for *EGFR* or *ALK* alterations using amplification refractory mutation system polymerase chain reaction and immunohistochemistry/fluorescence in situ hybridization. Molecular testing was extensively performed in patients with synchronous multifocal LUAC. Clonal evolution analysis was implemented using next-generation sequencing. **Results:** A total of 97 multiple synchronous lesions were observed among 1059 LUAC patients. Patients with at least 1 sample harboring *EGFR* mutation or *ALK* rearrangement were 62.89% (61/97) and 14.43% (14/97), respectively. Patients with concomitant *EGFR* and *ALK* alterations were 4.71% (4/97). Comparatively, patients with unifocal LUAC harboring *EGFR* mutation, *ALK* rearrangement, and *EGFR*/*ALK* co-alterations were 58.25% (570/962), 6.44% (62/962), and 0.83% (8/962), respectively. The prevalence of *EGFR*/*ALK* co-alterations in the multifocal LUAC was significantly higher than that in the unifocal LUAC (4.71% (4/97) vs. 0.83% (8/962)). Furthermore, we present 4 cases of *EGFR*/*ALK* co-altered multifocal LUAC with different morphological and molecular patterns. In addition to radiographic, pathological, and molecular testing results, clonal evolutional analysis could also be used to distinguish intertumoral heterogeneity. **Conclusion:** The results highlight the importance of distinguishing synchronous primary tumors from intrapulmonary metastases, and of assessing the relative abundance of *EGFR* mutation and *ALK* rearrangement in patients with multifocal adenocarcinomas with *EGFR*/*ALK* co-alterations.

Clinical Lung Cancer, Vol. 20, No. 4, e517-30

Keywords: Anaplastic lymphoma kinase rearrangement, Clonal evolution, Epidermal growth factor receptor, Intertumoral heterogeneity, Multifocal lung adenocarcinomas

J.F., X.D., and Z.W. contributed equally to this work.

[1]Department of Pathology
[2]Cancer Center
[3]Department of Radiology, Union Hospital, Tongji Medical College, Huazhong University of Science and Technology, Wuhan, Hubei, China
[4]Shanghai Tongshu Biotechnology Co, Ltd, Shanghai, China
[5]Clinical Institute for Lung Cancer, Mount Sinai Cancer, Mount Sinai Health System, Icahn School of Medicine at Mount Sinai, New York, NY

Submitted: Jan 31, 2019; Revised: Mar 5, 2019; Accepted: Apr 16, 2019; Epub: Apr 25, 2019

Addresses for correspondence: Xiu Nie, MD, Department of Pathology, Union Hospital, Tongji Medical College, Huazhong University of Science and Technology, 1277 Jiefang Ave, Wuhan, Hubei, China; or Fred R. Hirsch, MD, PhD, Clinical Institute for Lung Cancer, Mount Sinai Cancer, Mount Sinai Health System, One Gustave L. Levy Place-Box 1128, New York, NY 10029-6574
E-mail contact: 569050512@qq.com; Fred.Hirsch@mssm.edu

1525-7304/
https://doi.org/10.1016/j.cllc.2019.04.008

Introduction

With the widespread use of low-dose chest computed tomography (CT) and lung cancer screening, the reported incidence of lung cancer patients who present with multiple lesions ranges from 0.2% to 20%, particularly those of multiple lung adenocarcinomas (LUAC).[1-9] Many studies showed that intertumoral heterogeneity occurs in multifocal LUAC,[10-12] suggesting that most of these malignant lesions are genetically independent even occurring synchronously in a single patient. Concomitant epidermal growth factor receptor (*EGFR*) mutation and echinoderm microtubule-associated protein-like 4 (*EML4*) anaplastic lymphoma kinase (*ALK*) rearrangement have previously been reported to be approximately 1% in patients with non−small-cell lung cancer (NSCLC),[13-16] although *EML4-ALK* rearrangements initially were thought to be mutually exclusive with *EGFR*. The pattern of *EGFR* mutations and *EML4-ALK* rearrangements in multifocal LUAC can vary from one lesion to another.[17-19] So far most studies focused on intratumoral heterogeneity of *EGFR/ALK* co-altered LUAC.[20-23] However, few kinds of research have focused on the heterogeneity of *EGFR/ALK* co-altered LUAC. In this study, mutational status of *EGFR* and gene fusions in *EML4-ALK* was examined extensively in multiple synchronous LUAC from 1059 surgical resection LUAC. We also present the follow-up results of patients with multiple synchronous LUAC who had *EGFR* mutation and *EML4-ALK* fusion gene. We aimed to determine appropriate diagnostic and therapeutic strategies for dual-positive patients with multiple synchronous LUAC.

Patients and Methods

Patient Collection

A total of 1059 LUAC patients who underwent surgical resection were consecutively evaluated from September 2013 to January 2018 in the Union Hospital, Tongji Medical College, Huazhong University of Science and Technology, Hubei, China. We screened patients' mutational status of *EGFR* and *EML4-ALK*. A total of 97 patients had 231 surgically resected synchronous multifocal LUAC and 962 patients had unifocal LUAC. Clinical characteristics including age, sex, smoking history, histopathology, lesion size, lesion number, lesion location, and lesion stage were recorded. Tumor, node, metastases (TNM) staging was on the basis of the International Association for the Study of Lung Cancer eighth TNM lung cancer staging system. Morphological subtyping of LUAC was performed according to the 2015 World Health Organization classification criteria, with the percentage of each histologic component recorded in 5% increments (lepidic, acinar, papillary, micropapillary, and solid). The predominant pattern constituting the greatest percentage of tumor histopathologic findings was determined as the histopathologic subtype.

Immunohistochemistry and Fluorescence in Situ Hybridization

Anaplastic lymphoma kinase (D5F3) immunohistochemical staining was performed with OptiView DAB Detection Kits (Ventana Medical Systems, Roche Group, Tucson, AZ, USA) on BenchMark XT automated stainer (Ventana Medical Systems), following previously described procedures. Ventana anti-*ALK* (D5F3) rabbit monoclonal primary antibody has been approved by the US Food and Drug Administration (FDA) and China FDA for the identification of patients with NSCLC who are eligible for treatment with *ALK* tyrosine kinase inhibitors (TKIs). The assay was conducted with 4-μm thick formalin-fixed, paraffin-embedded (FFPE) tissue sections and each specimen had a negative and positive control. The *EML4-ALK* status of each case was assessed by 2 independent observers. All observers were unaware of the purpose of the study. Cases with discrepant *EML4-ALK* scores were further verified using fluorescence in situ hybridization (FISH) analysis. FISH analyses using Vysis *ALK* break-apart FISH probes (Abbott Molecular, Des Plaines, IL) were performed and evaluated according to the previously published methodology.

DNA Extraction

We performed DNA extraction from serial thick sections cut from tumor tissue samples and control sections. The invasive tumor content was estimated by pathologists, to ensure more than 50% of cells were tumor cells. The DNA was isolated from the FFPE using the DNeasy Blood and Tissue Kit (69504; Qiagen, Venlo, The Netherlands).

Epidermal Growth Factor Receptor Mutation Analysis

Epidermal growth factor receptor mutations were analyzed on the basis of the principle of the amplification refractory mutation system. Briefly, resected tumor samples were fixed in 10% neutral buffered formalin and embedded in paraffin wax. Extracted DNA was used for polymerase chain reaction (PCR) with the Mx3000PtM (Stratagene, La Jolla, CA) using the *EGFR* 29 Mutations Detection Kit (Amoy Diagnostics, Xiamen, China).

Next-Generation Sequencing

We created targeted capture pull-down and exon-wide libraries from native DNA using the xGen Exome Research Panel (Integrated DNA Technologies, Inc, Skokie, IL) and TruePrep DNA Library Prep Kit V2 for Illumina (TD501; Vazyme, Nanjing, China), and generated paired-end sequence data using Illumina HiSeq machines. The sequence data were aligned to the human reference genome (National Center for Biotechnology Information build 37) using Burrows-Wheeler Aligner.[24] GATK 4.0 was used to sort the aligned sequences and remove PCR duplication.[25] Somatic mutation calling was performed using Mutect1, Mutect2,[25] and VarDict.[26] Somatic mutations existing in at least 2 of the results of the 3 software were selected as high confident mutations. Copy number variations and loss of heterozygosity were analyzed using the CNVkit.[27] The subclonal architecture analysis was performed using sciClone.[28]

Statistical Analysis

Clinical characteristics were compared according to the *EGFR* or *EML4-ALK* status using the χ^2 test and Student *t* test. A 2-sided *P* value $< .05$ was defined as statistically significant. All analyses were performed using the SPSS software package (version 16.0; SPSS Inc, Chicago, IL).

Results

Patient Population

The flow chart of the research population and molecular testing results are presented in Figure 1A. Among 1059 patients, 97

patients had multiple intrapulmonary lesions, whose clinical characteristics are summarized in Table 1. Among these 97 patients, 71 patients had 2 intrapulmonary lesions and 26 patients had at least 3 pulmonary lesions.

Epidermal Growth Factor Receptor/ALK Status in Multifocal LUAC and Clinical Pathological Indicators

Overall distributions of *EGFR/ALK* status of 97 patients with multifocal LUAC are listed in Figure 1B. Sixty-one of 97 patients (62.89%) with at least 1 sample harboring *EGFR* mutation tended to be older and female without a significant smoking history (Table 2). Fourteen of 97 patients with at least 1 sample harboring *EML4-ALK* rearrangement tended to be younger at diagnosis with more tumor numbers and never-smoking history. Interestingly, *EML4-ALK* rearranged tumors showed higher lymph node metastasis, most commonly at stage N2 (Table 2).

Comparison of EGFR/ALK *Genetic Alterations in Unifocal/Multifocal LUAC*

Patients with unifocal LUAC were considered as a reference group and their clinical characteristics are listed in Supplemental Table 1 in the online version. *EGFR* mutation detected in patients with unifocal lesion (570/962, 59.25%) was not significantly different from that in patients with multifocal lesions (61/97, 62.89%; $P > .05$). *EML4-ALK* rearrangement detected in patients with multifocal lesions (14/97, 14.43%) was significantly higher than that in patients with unifocal lesion (62/962, 6.44%; Table 3).

Figure 1 The Flow Chart of the (A) Research Population and (B) Molecular Testing Results

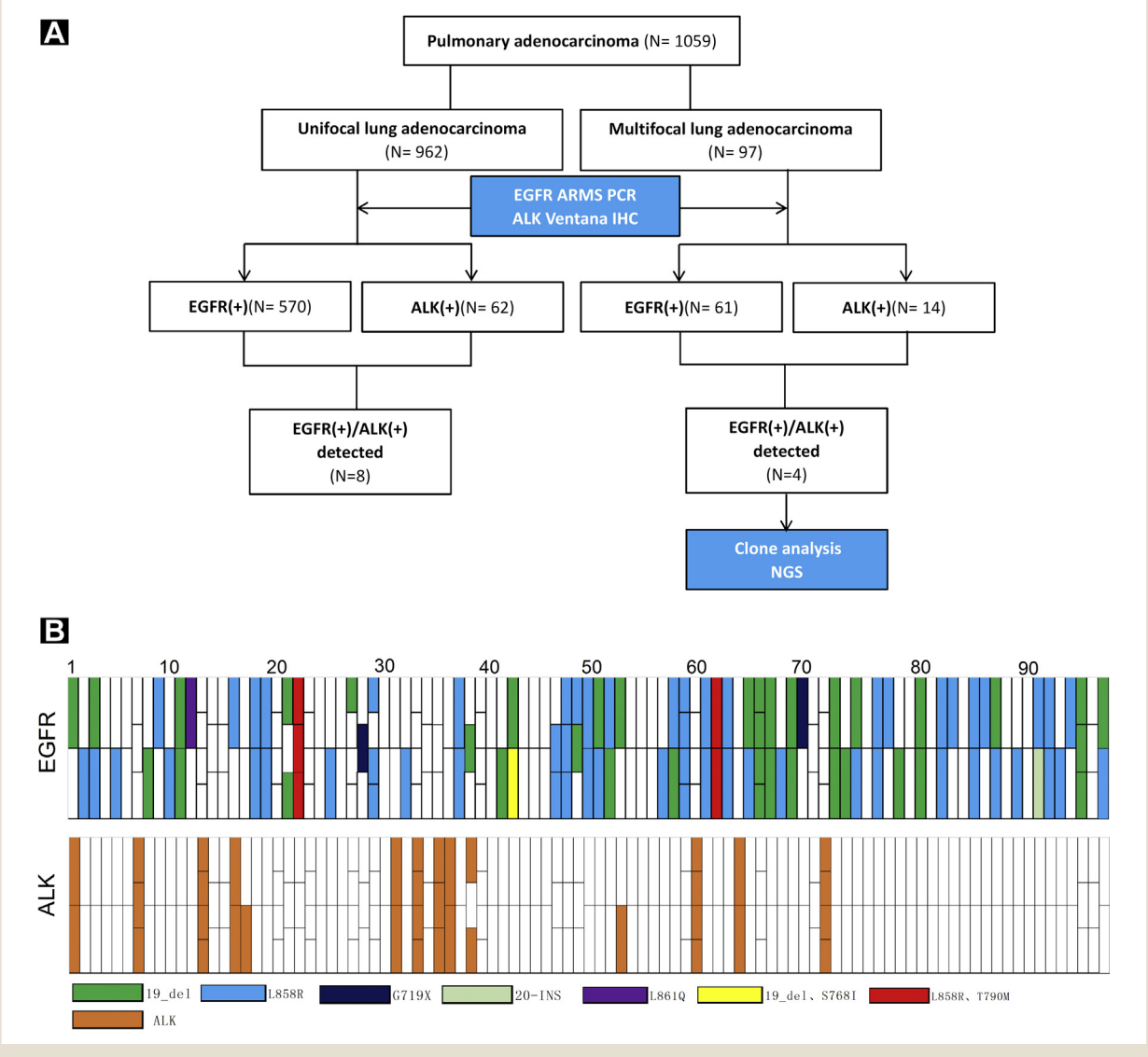

Abbreviations: ALK(+) = *ALK* rearrangement; ARMS = amplification refractory mutation system; EGFR(+) = *EGFR* mutation; IHC = immunohistochemistry; PCR = polymerase chain reaction.

Table 1 Clinical Characteristics of 97 Patients With Multifocal Lung Adenocarcinoma

Characteristic	Value
Mean Age ± SD, Years	56.13 ± 8.32
Sex	
Male	45 (46.39)
Female	52 (53.61)
Smoking Status	
Never Smokers	69 (71.13)
Ever Smokers	28 (28.87)
Largest Tumor Size (cm)	
≤3	73 (75.26)
3 to ≤5	18 (18.56)
5 to ≤7	5 (5.15)
>7	1 (1.03)
Lymph Node Metastasis	
Nx	38 (39.18)
N0	36 (37.11)
N1	2 (2.06)
N2	21 (21.65)
Tumor Numbers	
2	71 (73.20)
3	15 (15.46)
≥4	11 (11.34)
Tumor Location	
Unilateral same lobe	31 (31.96)
Unilateral different lobes	59 (60.82)
Bilateral	7 (7.22)
Stage	
II	14 (14.43)
III	31 (31.96)
IV	52 (53.61)
Resection Type	
Limited resection	40 (41.24)
Lobectomy and limited resection	24 (24.74)
Lobectomy	30 (30.93)
Pneumonectomy	3 (3.09)
Pleural Nodules	
0	51 (52.58)
1	46 (47.42)

Data are presented as n (%) except where otherwise noted.

Clinicopathological Characteristics of Patients With Multifocal LUAC Harboring Concomitant EGFR *Mutation and* EML4-ALK *Rearrangement*

The overall frequency of *EGFR*/*ALK* co-alterations in LUAC patients was 1.13% (12/1059). Of note, the prevalence of *EGFR*/*ALK* co-alterations in the multifocal LUAC patients was 4.17% (4/97), which was significantly higher than that in the unifocal LUAC patients (8/962; 0.83%; 95% confidence interval, 0.003-0.014; $P = .008$). The results indicated that driver alterations of *EGFR* and *EML4-ALK* could coexist in a small group of NSCLC, and more frequently in multifocal LUAC (Table 3).

Treatment Outcomes of Multifocal LUAC With EGFR/ALK *Co-alterations*

Case 1. Details of this case can be seen in the previous report.[29] Briefly, this patient was a 55-year-old non-smoker woman, whose CT scan showed a mass in the right upper lobe (1.8 × 1.2 cm) and a small nodule in the right lower lobe adjacent to the pleura (Figure 2B and G). After a right lower lobe wedge resection under video-assisted thoracic surgery (VATS), 3 spatially separated regions within the adenocarcinoma lesion were found (Figure 2L). Tumor 1 and tumor 2 showed a solid growth pattern and *EML4-ALK* rearrangement, whereas tumor 3 presented as an acinar pattern and *EGFR* mutation (Figure 2M-T). On the basis of the *EGFR* mutation, icotinib was orally administered at a dose of 125 mg 3 times per day. Unfortunately, 3 months later progressive disease was confirmed as the lesions enlarged slowly (Figure 2C and H), and icotinib therapy was stopped. Because of *EML4-ALK* rearrangement, the patient received crizotinib orally 250 mg twice a day for 2 months and showed a good response, which was evaluated as partial remission (Figure 2D and I). However, right pleural effusion occurred after 1 month. Then icotinib with crizotinib therapy was administered and the pleural effusion reduced gradually. The patient's condition was well controlled by *EGFR* and *ALK* TKIs for 1 year (Figure 2E and J). Then the patient relapsed with pericardial effusion and multiple pulmonary nodules (Figure 2F and K).

Case 2. Patient 2, a 57-year-old non-smoker woman, was sent to our hospital with dyspnea. A CT scan revealed a solid nodule in the left upper lobe (LUL; 3.2 cm × 3.9 cm; Figure 3B) and a ground-glass nodule in the left lower lobe (LLL; 2.3 × 1.6 cm; Figure 3C). The patient consequently underwent a LUL resection, a right lower lobe wedge resection, and VATS lymphadenectomy on July 27, 2017. The pathology confirmed invasive adenocarcinoma in the LUL lesion, with mixed solid and cribriform patterns (Figure 3E) and *EML4-ALK* rearrangement (Figure 3F and G), whereas *EGFR* mutation was negative (Figure 3H). The LLL nodule presented as invasive adenocarcinoma, with predominant papillary patterns (Figure 3I) and *EGFR* mutation (Figure 3L), whereas *EML4-ALK* rearrangement was negative (Figure 3J and K). All of the 6 metastatic lymph nodes showed a cribriform growth pattern, with *EML4-ALK* rearrangement rather than *EGFR* mutation (Figure 3M-P). The patient was diagnosed with pT2aN2M0. A first-line chemotherapy regimen of PP (pemetrexed 750 mg/m^2 with nedaplatin 110 mg/m^2) was carried out on August 26, 2017. After 6 cycles, the CT scan showed no signs of recurrence and lymphadenectasis. Then the patient was given chest radiotherapy with a dose of 54 Gy in 27 fractions. Six months later, the CT scan showed radiation pneumonitis in both lungs on February 28, 2018. The patient did not relapse until August 20, 2018.

Another 2 cases of multifocal LUAC with *EGFR*/*ALK* co-alterations are presented in Supplemental Appendix A in the online version.

Clonal Evolution Analysis

Exome sequencing was only performed on samples of patient 1 and patient 2 because of inadequate samples of patient 3 and patient 4. The result of somatic alterations of patient 1 and patient 2 showed that more than 73% of nonsynonymous mutations were

Table 2 Baseline Clinicopathologic Features of Multifocal Lung Adenocarcinoma Patients With *EGFR* Mutations or *ALK* Rearrangements

Characteristic	*EGFR*				*ALK*			
	EGFR Mutation	No *EGFR* Mutation	Total	*P*	*ALK* Rearrangement	No *ALK* Rearrangement	Total	*P*
Mean Age ± SD, Years	57.51 ± 7.11	53.81 ± 9.71	56.13 ± 8.32	.0335	49.29 ± 8.31	57.29 ± 7.79	56.13 ± 8.32	.0037
Sex								
Male	23	22	45	.026	6	39	45	.774
Female	38	14	52		8	44	52	
Smoking Status								
Never smoker	50	19	69	.002	14	55	69	.024
Ever smoker	11	17	28		0	28	28	
Largest Tumor Size (cm)								
≤3	50	23	73	.166	9	64	73	.029
3 to ≤5	9	9	18		2	16	18	
5 to ≤7	2	3	5		2	3	5	
>7	0	1	1		1	0	1	
Lymph Node Metastasis								
Nx	22	16	38		7	31	38	
N0	24	12	36	.887	1	35	36	.013
N1	1	1	2		0	2	2	
N2	14	7	21		6	15	21	
Tumor Number								
2	49	22	71	.039	7	64	71	.034
≥3	12	14	26		7	19	26	
Tumor Location								
Unilateral same lobe	12	19	31	.003	5	26	31	.947
Unilateral different lobes	44	15	59		8	51	59	
Bilateral	5	2	7		1	6	7	
Stage								
II	8	6	14	.521	0	14	14	.249
III	22	9	31		5	26	31	
IV	31	21	52		9	43	52	

Data are presented as n, except where otherwise noted.

Table 3 Comparison of Gene Status and Baseline Clinicopathologic Features in Unifocal and Multifocal Lung Adenocarcinoma

Characteristic	Lung Adenocarcinoma		*P*
	Unifocal	Multifocal	
Mean Age ± SD, Years	58.93 ± 8.78	56.13 ± 8.32	.0021
Sex			
Male	489	46	.522
Female	473	51	
Smoking Status			
Never smoker	637	69	.327
Ever smoker	325	28	
Lymph Node Metastasis			
Yes	288	23	.28
No	591	36	
Pleural Nodules			
0	273	46	<.001
1	689	51	
***ALK* Rearrangement**			
Yes	62	14	.004
No	900	83	
***EGFR* Mutation**			
Yes	570	61	.487
No	392	36	

Data are presented as n, except where otherwise noted.

unique in each tumor (see Supplemental Figure 3A in the online version). The genes that changed in at least 2 tumors are listed in Supplemental Figure 3B in the online version. The driver gene alterations are shown in Supplemental Figure 4 in the online version. We carried out a clonal evolution analysis for case 1 and case 2. Variant allele frequency (VAF) distributions are shown in Figure 2V and W and Figure 3Q. For case 1, the median VAFs for clusters 1 to 4 were 15.8%, 9.25%, 0.99%, and 8.9%, respectively, in tumor 1; and were 13.8%, 5.77%, 9.55%, and 0 in tumor 2, respectively (Figure 2V). As shown, most of the clusters were shared by tumor 1 and tumor 2 except cluster 4, which was exclusively in tumor 1, indicating that tumor 1 and 2 originated from the same clone. Three-dimensional analysis of tumor 1, 2, and 3 (Figure 2W) showed that tumor 3 was different from others although tumor 1 and 2 were similar. For case 2, the median VAFs for clusters 1 to 4 were 28.5%, 0, 13.5%, and 0, respectively, in tumor 1; and were 0.22%, 19.4%, 0, and 5.24% in tumor 2, respectively (Figure 3Q). That is, no clusters were shared by 2 tumors; and cluster 1 and 3 exclusively existed in tumor 1, whereas cluster 2 and 4 exclusively existed in tumor 2.

On the basis of the variant clustering results, we inferred that, for case 1, 1 of tumor 1 and tumor 2 was a metastatic lesion, but tumor 3 was a primary lesion. For case 2, tumor 1 and 2 were primary lesions.

Discussion

Multifocal LUACs are increasingly encountered in clinical practice and up to 8% of patients are diagnosed with multiple LUAC. With the introduction of precision-targeted therapy in NSCLC and the application of advanced molecular/genetic techniques, more *EGFR*/*ALK* co-altered NSCLC patients are identified. At present most studies have focused on intratumoral heterogeneity of *EGFR*/*ALK* co-altered LUAC.[20-23] Our studies pay more attention to intertumoral heterogeneity in multifocal LUAC with *EGFR*/*ALK* co-alterations. Mounting evidence has shown that the genetic instabilities of cancer cells cause genetic and phenotypic heterogeneity in the tumor, suggesting that different genetic alterations might occur in different tumor cells rather than a single clone.

Our results showed the prevalence of *EGFR*/*ALK* co-alterations in multifocal LUAC patients (4/97, 4.17%) was significantly higher than that in unifocal LUAC patients (8/962, 0.83%). Consistent with our results, Wu et al[30] reported that the rate of *EGFR*/*ALK* co-alterations in patients with synchronous multiple lung ground-glass opacity nodules was as high as 8.57%. In addition, they reported that patients with at least 1 driver mutation had a high inconsistency rate of 80%. Recently, Chen et al[31] reported a high inconsistency rate (89.7%) in genetic alterations between tumors within individual patients. Liu et al[32] studied the genomic profiles of 15 LUAC, which showed different genomic profiles, indicating that they were independent primary tumors. Therefore, our results are consistent with previous findings and support the hypothesis that multifocal adenocarcinoma lesions appear to be derived from different primary clonal lesions rather than from a single primary tumor. In that case, *EGFR*/*ALK* co-alterations are more prone to occur in patients with multifocal lesions because different genetic alterations might occur in different tumor cells rather than a single clone.

Treatment dilemma occurs when a patient presents with *EGFR*/*ALK* co-alterations. Current studies mostly focused on the responses to *EGFR* and/or *ALK* inhibitors in dual-positive mutation patients with unifocal adenocarcinoma. Lou et al[33] reported that first-line *EGFR*-TKI treatment might be appropriate for patients with advanced NSCLC harboring concomitant *EGFR* mutation and *EML4-ALK* rearrangement, but other studies suggested that *ALK* inhibitors could be used first for dual-positive patients, particularly those with low abundance of *EGFR* mutants. Few patients have been treated with *EGFR* and *ALK* inhibitors in the previous studies.[34] So far, there is no general consensus on the best treatment strategy for patients with *EGFR*/*ALK* co-alterations. In our study, the patient in case 1, whose resected lesion had 3 distinct tumors, 2 of which originated from the same clone driven by *ALK* rearrangement and 1 of which originated from a different clone driven by *EGFR* mutation, showed a poor response to first-line *EGFR*-TKI therapy with slow progression might be because of a low abundance of the *EGFR* mutation (2.2%), because *EGFR* abundance has been reported to be associated with the efficacy of *EGFR*-TKI therapy.[35] However, sequential *ALK*-TKI treatment for 2 months achieved a partial response and the lesion almost disappeared. As a consequence, we inferred that the unresected lesion in the right upper lobe was probably driven by *EML4-ALK* rearrangement. The patient's treatment process was tortuous, mainly because of complex tumor heterogeneity and high clinical stage. In contrast, the patient in case 2, who had 2 tumors that originated from different clones with *EGFR* mutation and *EML4-ALK* rearrangement, respectively, underwent only 6 cycles of platinum-based chemotherapy and chest

Figure 2 Illustration of Diagnosis and Therapy for Patient 1. (A) Treatment Timeline. (B-K) Computed Tomography Scans Before and After Treatment. (L) Results of Hematoxylin and Eosin (H&E) Staining Showed 3 Spatially Separated Regions (Tumor 1 [T1], Tumor 2 [T2], and Tumor 3 [T3]) on 1 Slide of the Adenocarcinoma Lesion. (M) T1 and T2 Presented a Solid Growth Pattern Using H&E Staining. (Q) T3 Presented an Acinar Pattern Using H&E Staining. (N and R) Results of Immunohistochemistry and Fluorescence in Situ Hybridization (O and S) Showed Positive Expression of *ALK* in T1 and T2 But Negative in T3. (P and T) Results of Amplification Refractory Mutation System Polymerase Chain Reaction Analysis Showed *EGFR* Mutation in T3 But not in T1 or T2. (U) The Model of 3 Spatially Separated Tumors in the Right Lower Lobe and 1 Tumor in the Right Upper Lobe. (V) Two-Dimensional Analysis of Tumor Subclonal Architecture of T1 and T2. (W) Three-Dimensional Analysis of Tumor Subclonal Architecture of T1, T2, and T3

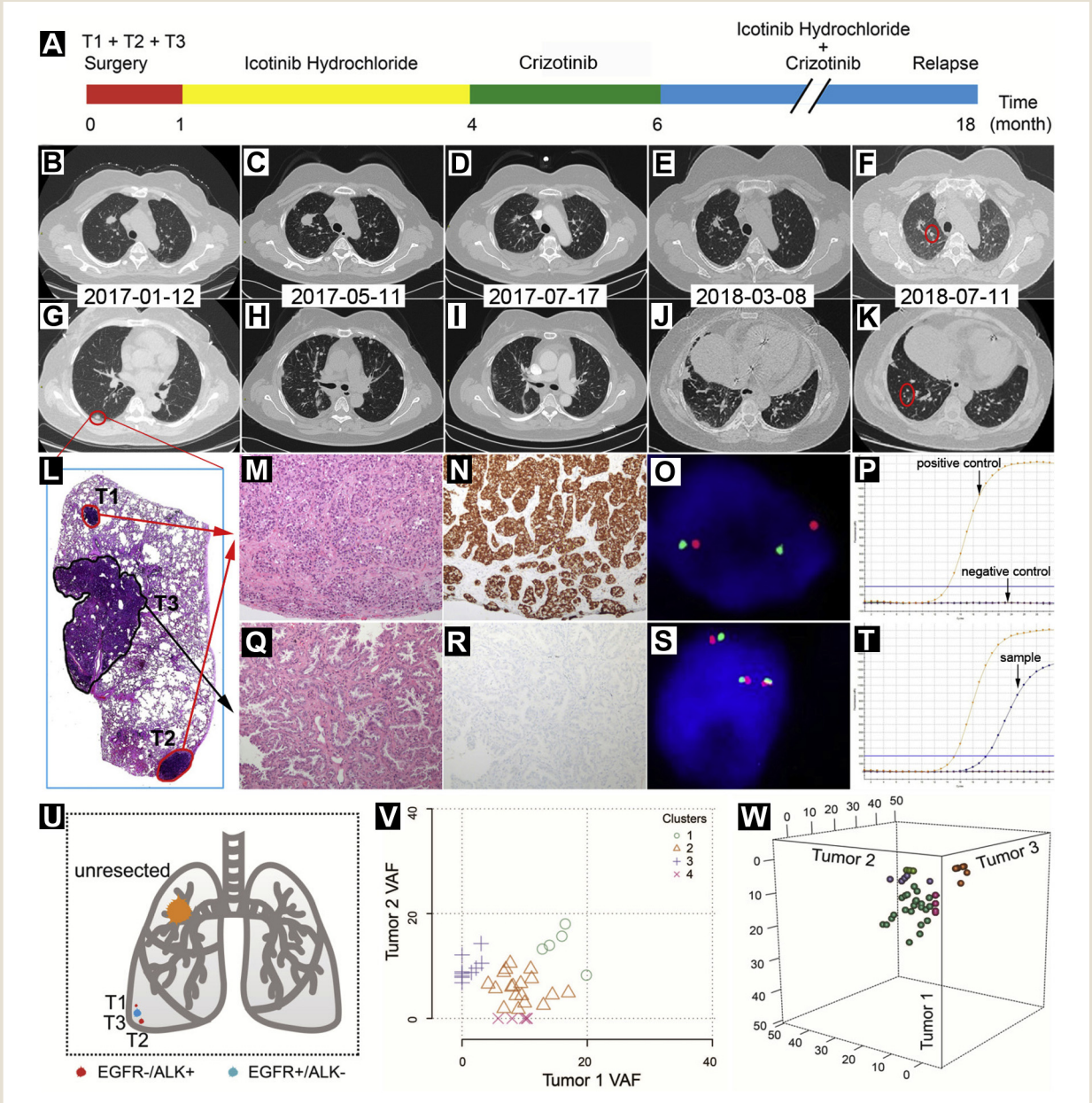

Abbreviation: VAF = variant allele frequency.

radiotherapy, however, progression-free survival (PFS) reached more than 1 year. This was mainly attributed to dual primary lesions and early clinical stage. By the way, in terms of treatment choices, China might be slightly different from the United States. Icotinib is a highly selective, first-generation *EGFR*-TKI, which is approved by the China FDA for the treatment for *EGFR* mutation-positive, advanced or metastatic NSCLC as first-line monotherapy in China. Icotinib was noninferior to gefitinib in terms of PFS and was

Figure 3 Illustration of Diagnosis and Therapy for Patient 2. (A) Treatment Timeline. Computed Tomography Scan of (B) Tumor 1 (T1) and (C) Tumor 2 (T2). (D) The Model of a Solid Nodule in the Left Upper Lobe and a Ground-Glass Nodule in the Left Lower Lobe. Results of Hematoxylin and Eosin (H&E) Staining Showed (E) Solid and Cribriform Patterns for T1 But (I) Papillary Patterns for T2. Results of Immunohistochemistry (IHC) and Fluorescence in Situ Hybridization (FISH) Showed Positive Expression of *ALK* in T1 (F and G, Respectively) But Negative in T2 (J and K, Respectively). Results of Amplification Refractory Mutation System Polymerase Chain Reaction (ARMS-PCR) Analysis Showed *EGFR* Mutation in (L) T2 But Not in (H) T1. Results of H&E Staining, IHC, FISH, and ARMS-PCR Analysis (M, N, O, and P, Respectively) Showed Cribriform Patterns, Positive Expression of *ALK*, and Negative *EGFR* Mutation, Respectively, in Metastatic Lymph Nodes. (Q) Two-Dimensional Analysis of Tumor Subclonal Architecture of T1 and T2

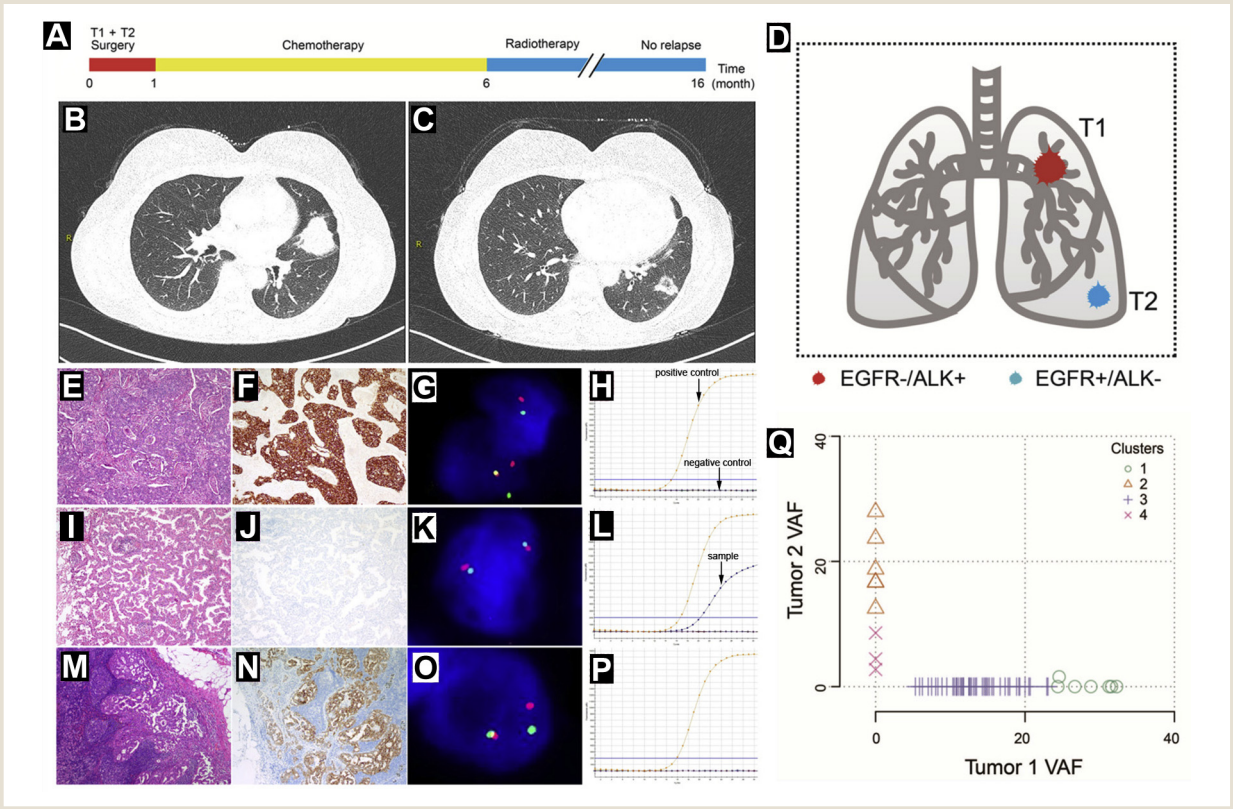

Abbreviation: VAF = variant allele frequency.

associated with fewer adverse events than gefitinib.[36] Platinum-based chemotherapy is the standard treatment for driver mutation-negative advanced NSCLC patients. In case 2, because of gastrointestinal toxicity, we chose nedaplatin instead of cisplatin.

The cases highlight the importance of distinguishing synchronous primary tumors from intrapulmonary metastases, and of assessing the relative abundance of *EGFR* mutation and *EML4-ALK* rearrangement in patients with multifocal adenocarcinomas with *EGFR/ALK* co-alterations. Furthermore, in 3 cases (case 2, case 3, and case 4) with lymph node metastasis, all metastatic lesions were driven by *ALK* rearrangement rather than *EGFR* mutation. This result suggests that *ALK* probably plays a key role in tumor metastasis.[37] However, more cases and research are needed to certify.

Conclusion

We found a high level of discrepancy in somatic-driven mutations in patients with multifocal LUAC, indicating that many tumors are likely to be independent primary rather than metastasis. We strongly advocate extensive molecular profiling in cases with multiple lesions to evaluate primary lesions or metastatic lesions. Herein we emphasize the importance of assessing the predominant driver gene to adopt the best treatment strategy. The optimal treatment strategy for these patients might depend on the clinical context and require communication between pathologists, laboratory technicians, and clinicians.

Clinical Practice Points

- The coexistence of *EGFR* mutation and *ALK* rearrangement in patients with multifocal LUAC constitutes a rare molecular subtype of lung cancer.
- Molecular testing and clonal evolutional analysis contributed to distinguishing primary tumors from intrapulmonary metastases.
- The optimal treatment strategy for patients with these tumors might depend on the clinical context and requires communication between pathologists, laboratory technicians, and clinicians.

Acknowledgments

This work was sponsored by Shanghai Tongshu Biotechnology Co.,Ltd and was supported in part by the National Natural Science Foundation of China (No. 81773022, No. 81602000).

Disclosure

The authors have stated that they have no conflicts of interest.

Supplemental Data

Supplemental figure, tables, and appendix accompanying this article can be found in the online version at https://doi.org/10.1016/j.cllc.2019.04.008.

References

1. Deschamps C, Pairolero PC, Trastek VF, Payne WS. Multiple primary lung cancers. Results of surgical treatment. *J Thorac Cardiovasc Surg* 1990; 99:769-77 [discussion: 777-778].
2. Verhagen AF, Tavilla G, van de Wal HJ, Cox AL, Lacquet LK. Multiple primary lung cancers. *Thorac Cardiovasc Surg* 1994; 42:40-4.
3. Carey FA, Donnelly SC, Walker WS, Cameron EW, Lamb D. Synchronous primary lung cancers: prevalence in surgical material and clinical implications. *Thorax* 1993; 48:344-6.
4. Pommier RF, Vetto JT, Lee JT, Johnston KM. Synchronous non—small-cell lung cancers. *Am J Surg* 1996; 171:521-4.
5. Nakata M, Sawada S, Yamashita M, et al. Surgical treatments for multiple primary adenocarcinoma of the lung. *Ann Thorac Surg* 2004; 78:1194-9.
6. Chang YL, Wu CT, Lee YC. Surgical treatment of synchronous multiple primary lung cancers: experience of 92 patients. *J Thorac Cardiovasc Surg* 2007; 134:630-7.
7. Aguiló R, Macià F, Porta M, Casamitjana M, Minguella J, Novoa AM. Multiple independent primary cancers do not adversely affect survival of the lung cancer patient. *Eur J Cardiothorac Surg* 2008; 34:1075-80.
8. Kim TJ, Goo JM, Lee KW, Park CM, Lee HJ. Clinical, pathological and thin-section CT features of persistent multiple ground-glass opacity nodules: comparison with solitary ground-glass opacity nodule. *Lung Cancer* 2009; 64:171-8.
9. Arai J, Tsuchiya T, Oikawa M, et al. Clinical and molecular analysis of synchronous double lung cancers. *Lung Cancer* 2012; 77:281-7.
10. De Sousa E Melo F, Vermeulen L, Fessler E, Medema JP. Cancer heterogeneity–a multifaceted view. *EMBO Rep* 2013; 14:686-95.
11. Yang D, Denny SK, Greenside PG, et al. Intertumoral heterogeneity in SCLC is influenced by the cell type of origin. *Cancer Discov* 2018; 8:1316-31.
12. Pozo K, Kelenis DP, Minna JD, Johnson JE. Different originating cells underlie intertumoral heterogeneity in lung neuroendocrine tumors. *Cancer Discov* 2018; 8:1216-8.
13. Santelmo C, Ravaioli A, Barzotti E, et al. Coexistence of EGFR mutation and ALK translocation in NSCLC: literature review and case report of response to gefitinib. *Lung Cancer* 2013; 81:294-6.
14. Baldi L, Mengoli MC, Bisagni A, Banzi MC, Boni C, Rossi G. Concomitant EGFR mutation and ALK rearrangement in lung adenocarcinoma is more frequent than expected: report of a case and review of the literature with demonstration of genes alteration into the same tumor cells. *Lung Cancer* 2014; 86:291-5.
15. Caliez J, Monnet I, Pujals A, et al. Lung adenocarcinoma with concomitant EGFR mutation and ALK rearrangement [in French]. *Rev Mal Respir* 2017; 34:576-80.
16. Ulivi P, Chiadini E, Dazzi C, et al. Nonsquamous, non—small-cell cancer patients who carry a double mutation of EGFR, EML4-ALK or KRAS: frequency, clinical-pathological characteristics, and response to therapy. *Clin Lung Cancer* 2016; 17:384-90.
17. Liu M, He WX, Song N, Yang Y, Zhang P, Jiang GN. Discrepancy of epidermal growth factor receptor mutation in lung adenocarcinoma presenting as multiple ground-glass opacities. *Eur J Cardiothorac Surg* 2016; 50:909-13.
18. Yoshida A, Tsuta K, Nakamura H, et al. Comprehensive histologic analysis of ALK-rearranged lung carcinomas. *Am J Surg Pathol* 2011; 35:1226-34.
19. Nishino M, Klepeis VE, Yeap BY, et al. Histologic and cytomorphologic features of ALK-rearranged lung adenocarcinomas. *Mod Pathol* 2012; 25:1462-72.
20. Li Y, Su S, Cai G, et al. Responses to crizotinib and chemotherapy in patients with lung adenocarcinoma harboring a concomitant EGFR mutation and ALK gene rearrangement: a case report and review of the literature. *Mol Clin Oncol* 2017; 7:173-82.
21. Jamal-Hanjani M, Wilson GA, McGranahan N, et al. Tracking the evolution of non—small-cell cancer. *N Engl J Med* 2017; 376:2109-21.
22. Crockford A, Jamal-Hanjani M, Hicks J, Swanton C. Implications of intratumour heterogeneity for treatment stratification. *J Pathol* 2014; 232:264-73.
23. Cai W, Lin D, Wu C, et al. Intratumoral heterogeneity of ALK-rearranged and ALK/EGFR coaltered lung adenocarcinoma. *J Clin Oncol* 2015; 33:3701-9.
24. Slater PM, Grivell R, Cyna AM. NGS-1 labour management of a woman with carnitine palmitoyl transferase type 2 deficiency. *Anaesth Intensive Care* 2009; 37:305-8.
25. McKenna A, Hanna M, Banks E, et al. NGS-2 The Genome Analysis Toolkit: a MapReduce framework for analyzing next-generation DNA sequencing data. *Genome Res* 2010; 20:1297-303.
26. Lai Z, Markovets A, Ahdesmaki M, et al. NGS-3 VarDict: a novel and versatile variant caller for next-generation sequencing in cancer research. *Nucleic Acids Res* 2016; 44:e108.
27. Talevich E, Shain AH, Botton T, Bastian BC. NGS-4 CNVkit: genome-wide copy number detection and visualization from targeted DNA sequencing. *PLoS Comput Biol* 2016; 12:e1004873.
28. Miller CA, White BS, Dees ND, et al. NGS-5 SciClone: inferring clonal architecture and tracking the spatial and temporal patterns of tumor evolution. *PLoS Comput Biol* 2014; 10:e1003665.
29. Fan J, Dai X, Nie X. Concomitant epidermal growth factor receptor mutation and EML4-ALK fusion in a patient with multifocal lung adenocarcinomas. *J Thorac Oncol* 2018; 13:e45-8.
30. Wu C, Zhao C, Yang Y, et al. High discrepancy of driver mutations in patients with NSCLC and synchronous multiple lung ground-glass nodules. *J Thorac Oncol* 2015; 10:778-83.
31. Chen K, Chen W, Cai J, et al. Favorable prognosis and high discrepancy of genetic features in surgical patients with multiple primary lung cancers. *J Thorac Cardiovasc Surg* 2018; 155:371-9.e1.
32. Liu Y, Zhang J, Li L, et al. Genomic heterogeneity of multiple synchronous lung cancer. *Nat Commun* 2016; 7:13200.
33. Lou NN, Zhang XC, Chen HJ, et al. Clinical outcomes of advanced non—small-cell lung cancer patients with EGFR mutation, ALK rearrangement and EGFR/ALK co-alterations. *Oncotarget* 2016; 7:65185-95.
34. Won JK, Keam B, Koh J, et al. Concomitant ALK translocation and EGFR mutation in lung cancer: a comparison of direct sequencing and sensitive assays and the impact on responsiveness to tyrosine kinase inhibitor. *Ann Oncol* 2015; 26:348-54.
35. Zhou Q, Zhang XC, Chen ZH, et al. Relative abundance of EGFR mutations predicts benefit from gefitinib treatment for advanced non—small-cell lung cancer. *J Clin Oncol* 2011; 29:3316-21.
36. Shi Y, Zhang L, Liu X, et al. Icotinib versus gefitinib in previously treated advanced non—small-cell lung cancer (ICOGEN): a randomised, double-blind phase 3 non-inferiority trial. *Lancet Oncol* 2013; 14:953-61.
37. Seto K, Kuroda H, Yoshida T, et al. Higher frequency of occult lymph node metastasis in clinical N0 pulmonary adenocarcinoma with ALK rearrangement. *Cancer Manag Res* 2018; 10:2117-24.

Case 3 Patient 3

A 50-year-old man whose CT scan showed a small nodule in the LUL (see Supplemental Figure 1A in the online version) and a solid nodule in the LLL (see Supplemental Figure 1E in the online version) underwent an LLL resection. The pathology confirmed invasive adenocarcinoma in the LUL lesion, with prevalent solid patterns (see Supplemental Figure 1B in the online version) and *EML4-ALK* rearrangement (see Supplemental Figure 1C in the online version), whereas *EGFR* mutation was negative (see Supplemental Figure 1D in the online version). The LLL nodule presented as invasive mucinous adenocarcinoma, with predominant signet-ring cell patterns (see Supplemental Figure 1F in the online version) and *EGFR* mutation (see Supplemental Figure 1H in the online version), whereas *EML4-ALK* rearrangement was negative (see Supplemental Figure 1G in the online version). Metastatic lymph nodes showed solid patterns, with *EML4-ALK* rearrangement rather than *EGFR* mutation (see Supplemental Figure 1I-L in the online version). The patient was diagnosed with pT2aN2M0. A first-line chemotherapy regimen (docetaxel 750 mg/m^2 with nedaplatin 110 mg/m^2) was carried out for 4 cycles from February, 2015. A CT scan on December 22, 2016 showed an intracranial space-occupying lesion, suggesting likely brain metastasis. The patient underwent intensity-modulated radiotherapy for brain metastases on February 8, 2017 and chemotherapy (docetaxel 750 mg/m^2 with nedaplatin 110 mg/m^2) for 3 cycles from September 1, 2017. The patient has remained stable up to now.

Case 4 Patient 4

A 57-year-old man whose positron emission tomography-CT scan showed a nodule (6 × 5 cm) with mediastinum, left hilar lymph node, and thoracic 1 vertebral body metastasis in the LLL (see Supplemental Figure 2E in the online version) and a nodule (0.2 × 0.1 cm) in the LUL (see Supplemental Figure 2A in the online version) underwent a LLL resection, LUL nodule resection, pulmonary mediastinal lymph node dissection, and intercostal nerve cryoablation. The pathology confirmed invasive adenocarcinoma in the LUL lesion, with predominant solid patterns (see Supplemental Figure 2B in the online version), *EML4-ALK* rearrangement (see Supplemental Figure 2C in the online version) and *EGFR* mutation (see Supplemental Figure 2D in the online version); and invasive adenocarcinoma in the LLL lesion, with solid patterns (see Supplemental Figure 2F in the online version) and *EML4-ALK* rearrangement (see Supplemental Figure 2G in the online version), whereas *EGFR* mutation was negative (see Supplemental Figure 2H in the online version). Metastatic lymph nodes showed solid patterns, with EML4-ALK rearrangement rather than EGFR mutation (see Supplemental Figure 2I-L in the online version). The patient was diagnosed with pT2aN2M0. A first-line chemotherapy regimen (pemetrexed 750 mg/m^2 with nedaplatin 110 mg/m^2) was carried out for 4 cycles from August 10, 2013. Meanwhile, the C7 to T2 vertebral body was treated with concurrent radiotherapy (30 Gy in 10 fractions) on August 14, 2013. Then chemotherapy with only pemetrexed (750 mg/m^2) was given for 1 cycle on November 21, 2013. A CT scan showed brain metastasis, and whole-brain radiotherapy (30 Gy in 10 fractions) followed by local focal contractile radiotherapy (30 Gy in 10 fractions) was carried out. From June 2014, the patient was given crizotinib 250 mg (2 months later, 200 mg) orally twice per day. The patient's condition was evaluated as stable disease according to the CT scan in November 2015. Magnetic resonance plain and enhanced scans showed an increased range of brain metastases in February 2016. The patient died in January 2017.

Supplemental Figure 1 Radiographic, Pathological, and Molecular Testing Results of Patient 3. (A and E) Computed Tomography Scan of Tumor 1 and 2, Respectively. A: The *red arrow* indicates the small nodule in the LUL. Results of Hematoxylin and Eosin (H&E) Staining Showed Solid Patterns for Tumor 1 (B) But Signet-Ring Cell Patterns for Tumor 2 (F). Results of Immunohistochemistry (IHC) Showed Positive Expression of ALK in Tumor 1 (C) But Negative in Tumor 2 (G). Results of Amplification Refractory Mutation System Polymerase Chain Reaction (ARMS-PCR) Showed *EGFR* Mutation in Tumor 2 (H) But Not in Tumor 1 (D). Results of H&E Staining (I, Magnification ×40; J, Magnification ×100), IHC (K), and ARMS-PCR (L) Showed Solid Patterns, Positive Expression of *ALK* and Negative *EGFR* Mutation, Respectively, in Metastatic Lymph Nodes

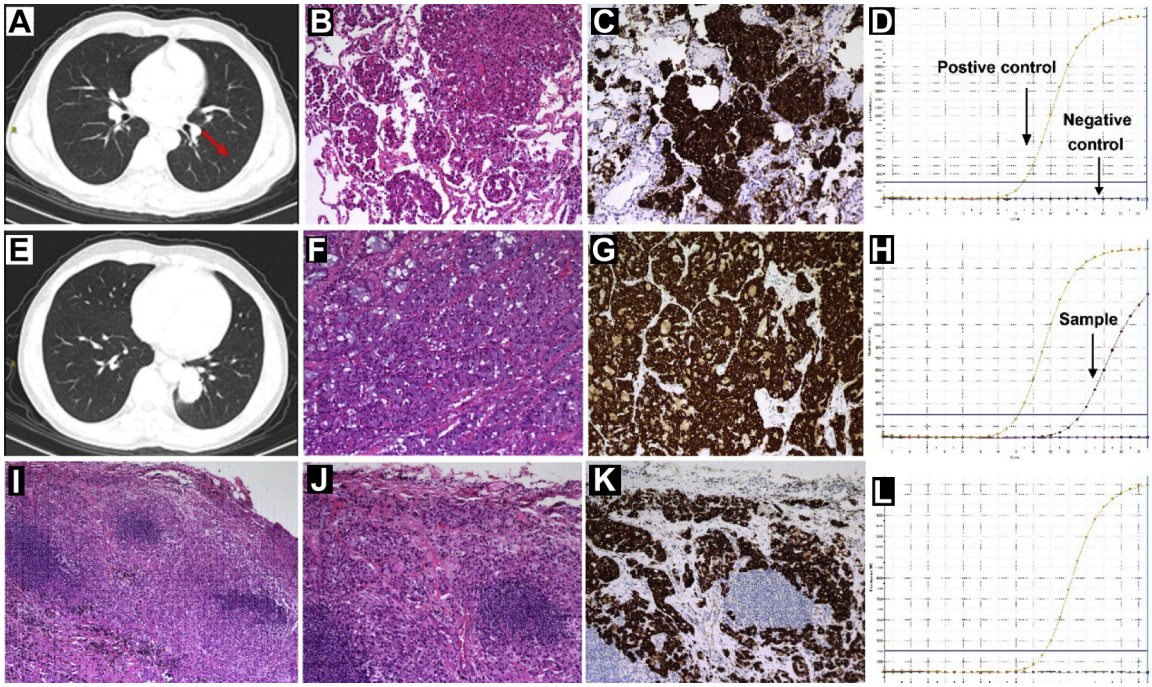

Supplemental Figure 2 Radiographic, Pathological, and Molecular Testing Results of Patient 4. (A and E) Computed Tomography Scan of Tumor 1 and 2, Respectively. A: The *red arrow* indicates the small nodule in the LUL. (B and F) Results of Hematoxylin and Eosin (H&E) Staining Showed Solid Patterns for Tumor 1 and Tumor 2, Respectively. (C and G) Results of Immunohistochemistry (IHC) Showed Positive Expression of *ALK* in Tumor 1 and Tumor 2, Respectively. Results of Amplification Refractory Mutation System Polymerase Chain Reaction (ARMS-PCR) Showed (D) *EGFR* Mutation in Tumor 1 But (H) Not in Tumor 2. Results of (I) H&E Staining, (J) IHC, (K) Fluorescence in Situ Hybridization, and (L) Amplification Refractory Mutation System Polymerase Chain Reaction Showed Solid Patterns, Positive Expression of *ALK*, and Negative *EGFR* Mutation, Respectively, in Metastatic Lymph Nodes

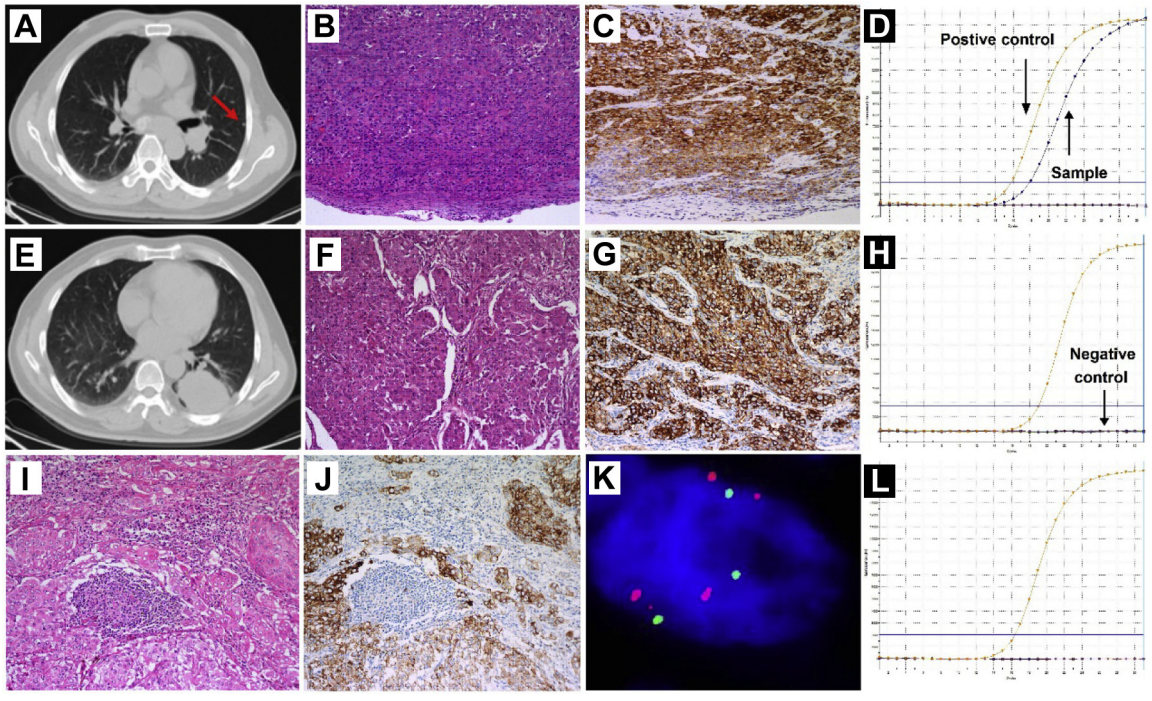

Supplemental Figure 3 Nonsynonymous Somatic Mutations (SNVs and Indels) in Tumor 1, Tumor 2, and Tumor 3 of Patient 1, and in Tumor 1 and Tumor 2 of Patient 2. (A) Numbers of Somatic Mutations. (B) Gene Mutations Shared by Different Tumors

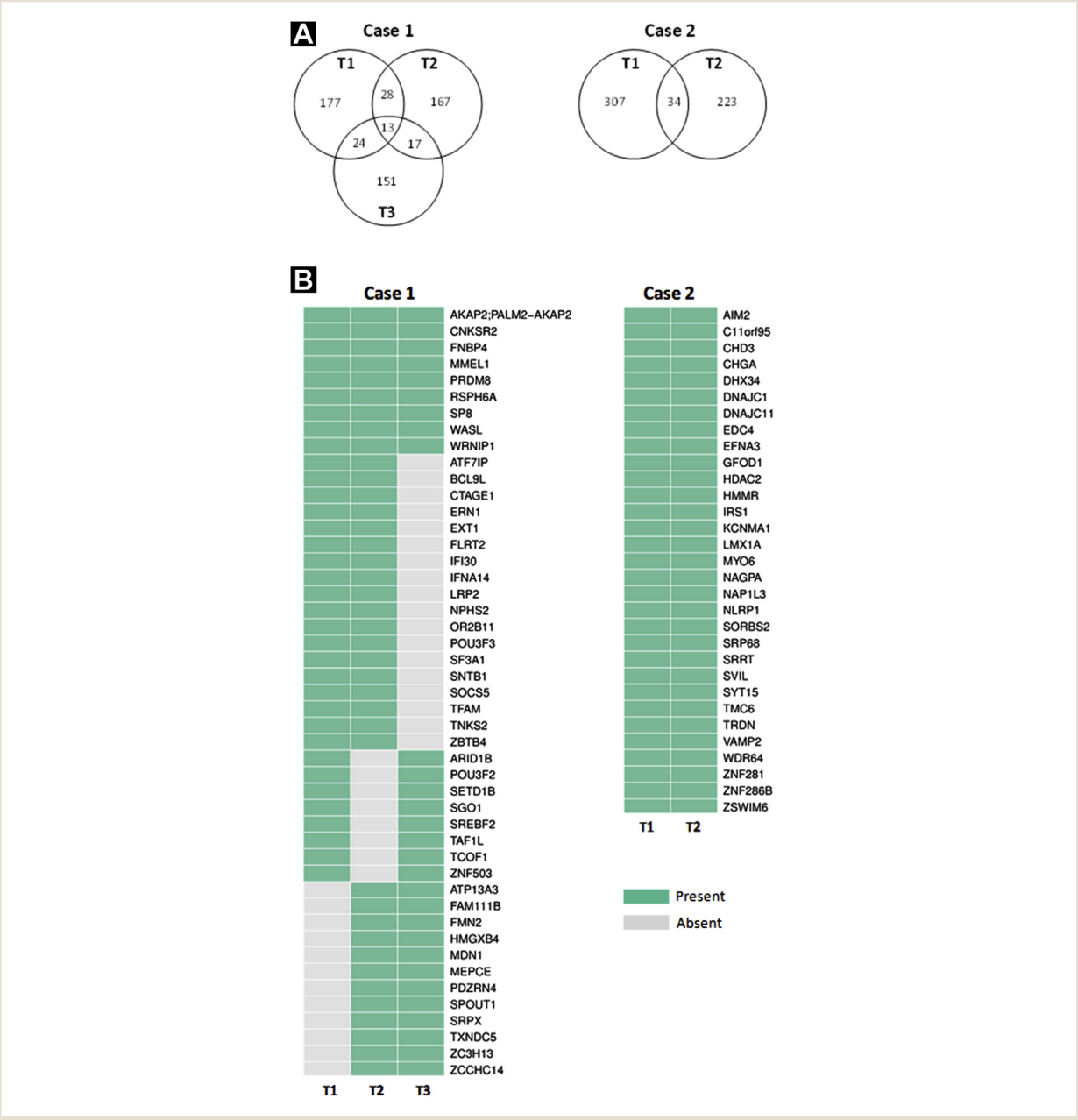

Abbreviation: SNVs = single nucleotide variants.

Supplemental Figure 4 Driver Gene Mutations in (A) Tumor 1, Tumor 2, and Tumor 3 of Patient 1, and (B) in Tumor 1 and Tumor 2 of Patient 2

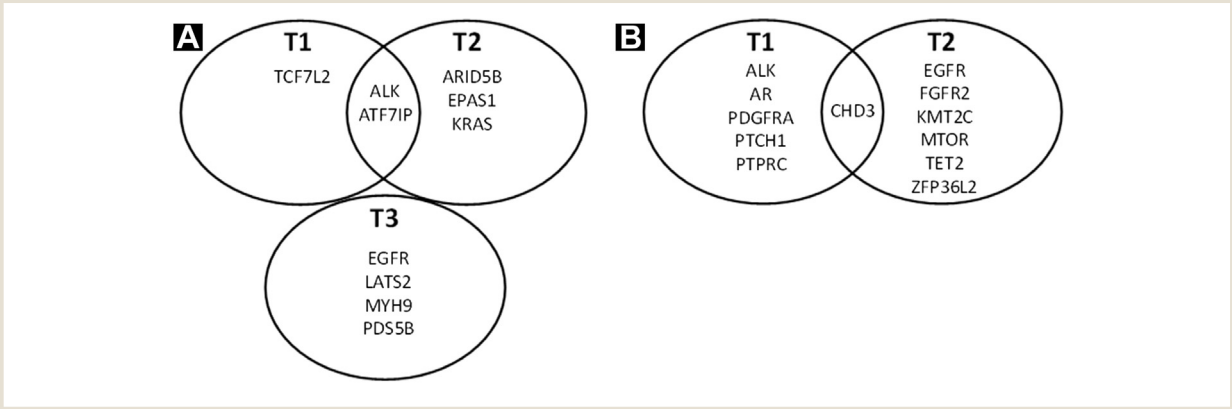

Supplemental Table 1 Clinical Characteristics of 962 Patients With Unifocal Lung Adenocarcinoma

Characteristic	*EGFR*			*ALK*			Total
	EGFR Mutation	No *EGFR* Mutation	*P*	*ALK* Rearrangement	No *ALK* Rearrangement	*P*	
Mean Age ± SD	59.18 ± 8.79	58.57 ± 8.77	.29	53.95 ± 9.13	59.28 ± 8.66	<.001	58.93 ± 8.78
Sex							
Male	231	258	<.001	23	466	.025	489
Female	339	134		39	434		473
Smoking Status							
Never Smoker	442	195	<.001	43	594	.589	637
Ever Smoker	128	197		19	306		325
Largest Tumor Size (cm)							
≤3	311	206	.003	33	484	.959	517
3 to ≤5	209	129		23	315		338
5 to ≤7	44	39		5	78		83
>7	6	18		1	23		24
Lymph Node Metastasis							
Nx	51	31		8	74		82
N0	347	245	.735	30	562	.071	592
N1	21	11		1	31		32
N2	151	105		23	233		256
Stage							
I	252	167	.026	22	397	.105	419
II	28	32		2	58		60
III	86	78		17	147		164
IV	173	99		18	254		272

Data are presented as n except where otherwise noted.